

# Particle modeling of disk-shaped galaxies of stars on nowadays concurrent supercomputers

Evgeny Griv\*, Michael Gedalin, Edward Liverts and David Eichler  
*Department of Physics, Ben-Gurion University of the Negev, P.O. Box 653,  
 Beer-Sheva 84105, Israel*

Yehoshua Kimhi  
*High Performance Computing Unit, Inter University Computational Center, Tel  
 Aviv University, Ramat Aviv 69978, Israel*

Chi Yuan  
*Academia Sinica Institute of Astronomy and Astrophysics (ASIAA), P.O. Box  
 1-87 Nankang, Taipei 11529, Taiwan*

**Abstract.** The time evolution of initially balanced, rapidly rotating models for an isolated disk of highly flattened galaxies of stars is calculated. The method of direct integration of the Newtonian equations of motion of stars over a time span of many galactic rotations is applied. Use of modern concurrent supercomputers has enabled us to make long simulation runs using a sufficiently large number of particles  $N = 30,000$ . One of the goals of the present simulation is to test the validities of a modified local criterion for stability of Jeans-type gravity perturbations (e.g. those produced by a barlike structure, a spontaneous perturbation and/or a companion galaxy) in a self-gravitating, infinitesimally thin and collisionless disk. In addition to the local criterion we are interested in how model particles diffuse in velocity. This is of considerable interest in the kinetic theory of stellar disks. Certain astronomical implications of the simulations to actual disk-shaped (i.e. rapidly rotating) galaxies are explored. The weakly nonlinear, or quasi-linear kinetic theory of the Jeans instability in disk galaxies of stars is described as well.

**Keywords:** Galaxies: kinematics and dynamics, galaxies: spiral, galaxies: physical properties, instabilities and waves.

**JEL codes:** will be inserted by the editor

## 1. Introduction

In galactic astronomy, the most intensely studied of the problems of pattern formation is the problem of the formation of spiral structure, which has brought forth numerous theoretical and numerical approaches. Even though at the present time there exists, as yet, no satisfactory theory of the origin and conservation of the spiral structure so prominent in the Milky Way and many other giant flattened galaxies, the majority of experts in the field has yielded to the opinion that the

---

\* Corresponding author (email: griv@bgumail.bgu.ac.il).



study of the stability of the small-amplitude cooperative oscillations in disk-shaped galaxies of stars is the first step towards an understanding of the phenomena. This is because in the Milky Way and many other disk galaxies, the bulk of the luminous mass, probably  $\gtrsim 90\%$ , is in the stars. Therefore, it seems likely that the spiral structures are intimately connected with the stellar constituent of a galaxy, and that stellar dynamical phenomena play a basic role. Because of the long-range nature of the gravitational force between stars, a galaxy exhibits collective modes of motions — modes in which the stars in large regions move coherently or in unison. A galaxy is characterized also by a high “temperature” (a dispersion of random velocities of stars) and hence a high “thermal” energy; this thermal energy is much larger than the interaction potential between pairs of stars. Because of this, binary encounters produce only small-scale scattering of the motions of the stars. Over long enough times, these gradually build up to produce large deflections that constitute collisions. In many cases these collisional effects are so weak that we consider the galaxy as collisionless on the Hubble time  $T \sim 10^{10}$  yr (Chandrasekhar, 1960; Binney and Tremaine, 1987). Thus, the galaxy is dominated by the collective motions and the free streaming of the stars (kinetic effects).

As usual it is very difficult to determine a priori whether a particular linearization of nonlinear equations made in analytical studies constitutes a valid approximation. This can be determined, however, by direct computer simulations of the nonlinear theory that mimic the behaviour of stars in galaxies. Such modeling gives more detailed information than can be obtained analytically, so that the important physical phenomena can be determined. In this paper, the results of the approximate theoretical analysis described in the Appendix are compared with our own many-body ( $N$ -body) simulations. One of the goals of the simulation is to test the validities of a modified local criterion for stability of Jeans-type gravity perturbations in a self-gravitating, infinitesimally thin and collisionless disk. The fact that the nonaxisymmetric perturbations in the differentially rotating system are more unstable than the axisymmetric ones is taken into account in this modified Toomre-like (Toomre, 1964, 1977) criterion.

In addition to the stability criterion we are interested in how model particles diffuse in velocity. As for the present study, such random velocity diffusion is caused by stellar disk turbulence. In particular, we verify the analytical prediction that as the Jeans-unstable perturbations grow the mean-square velocity increases linearly with time. The observation of this behavior is a sensitive test of the model as well as the kinetic theory of stellar disks.

In fact, Morozov (1981) and Griv *et al.* (1999a) already attempted to confirm the modified criterion numerically. However, because of the very small number of model stars,  $N = 200$ , Morozov's results are subject to considerable uncertainties, and additional simulations are clearly required to settle the issue. Furthermore, for that number of model particles, the two-body relaxation time scale is comparable to the crossing time, even with Morozov's modest softening parameter, raising some question about the applicability of his simulations to actual almost collisionless galaxies. Increasing the number of model stars is definitely a more reliable procedure. In turn, Griv *et al.* used a different numerical approach of the so-called local  $N$ -body simulations. The  $N$ -body experiments in a local or Hill's approximation has been pioneered by Toomre (1990), Toomre and Kalnajs (1991) and Salo (1995). In these simulations dynamics of particles in small regions of the disk are assumed to be statistically independent of dynamics of particles in other regions. The local numerical model thus simulates only a small part of the system and more distant parts are represented as copies of the simulated region. Unlike Morozov (1981) and Griv *et al.* (1999a), we study some aspects of dynamical behavior of stellar systems by global simulations using a sufficiently large number of particles.

## 2. $N$ -body simulations

Different methods are currently employed to simulate global evolution of collisionless point-mass systems of galaxies by  $N$ -body experiments. One algorithm for a simulation code that has found wide use was developed by Hohl and Hockney (1969), Hohl (1971, 1972), Miller (1971), Hockney and Brownrigg (1974), Quirk (1972), Athanassoula and Sellwood (1986), Combes *et al.* (1990), Pfenniger and Friedli (1993), Merritt and Sellwood (1994), Donner and Thomasson (1994), and others. The method samples the density field with a usually uniform grid. The Poisson equation is then solved on this grid using one of a number of the fast solvers that are available, usually Fast Fourier Transforms. This is an analog of plasma particle-in-cell (PIC) codes. It is believed that simulating many billions of stars in actual galaxies by using only several ten or hundred thousands representative stars in PIC experiments will be enough to capture the essential physics, which includes the ordinary star–star binary relaxation and wave-like collective motion. In other fields, such as the simulation of spiral structures, PIC codes may be used with moderate success. This is because these fine-scale  $\lesssim 1$  kpc structures can basically be governed by collisionless processes. By increasing the number of cells to reproduce the microstructures, one

reduces the average number of particles per cell, and thus increases the undesirable effect of particle gravitational encounters. In addition, if one uses PIC codes, then one cannot resolve density fluctuations with wavelengths smaller than the size of a cell  $d$ . This puts a lower limit on the wavelengths that it makes any sense to keep; this lower limit is given by  $\lambda_{\min} \approx d$ . Other disadvantages of PIC codes are possibilities of late-time loss of energy conservation, finite-grid and aliasing instabilities, and other numerical artifacts.

PIC method works well only for regions where there are many particles per cell. The problem is serious because there are regions in the phase space which are important to the problem but in which the distribution function is small. In general, since we will at most have a hundred particles in one cell we will have fluctuation of the order of 10% or more which for many problems is unacceptable.

In another type of  $N$ -body simulation, Ostriker and Peebles (1973), Morozov (1981), Grivnev (1985), Griv *et al.* (1994), Griv and Zhytnikov (1995), Griv and Chiueh (1998) investigated a stellar disk by direct integration of Newtonian equations of motion. Following them, we simulate here the evolution of a model for an isolated thin disk of a galaxy by direct integration of the equations of motion of stars: the force on a star  $i$  due to all other stars is given by

$$\frac{d^2 \mathbf{r}_i}{dt^2} = G \sum_{j \neq i}^N \frac{m_i m_j (\mathbf{r}_j - \mathbf{r}_i)}{[(\mathbf{r}_j - \mathbf{r}_i)^2 + r_{\text{cut}}^2]^{3/2}}, \quad (1)$$

where  $G$  is the constant of gravitation,  $m_i$ ,  $m_j$ ,  $\mathbf{r}_i$  and  $\mathbf{r}_j$  are the mass, position and velocity of the  $i$ -th and of the  $j$ -th particle, respectively, and  $r_{\text{cut}}$  is the so-called cutoff radius. This “softening” of the gravitational potential is a device often used in  $N$ -body simulations to avoid numerical difficulties at very close but rare encounters (Miller, 1971; Romeo, 1998). The constant parameter  $r_{\text{cut}}$  reduces the interaction at short ranges and puts a lower limit on the size of the particles, i.e. the stars in the system can no longer be considered as point-masses — they are in fact Plummer spheres with a scale size  $r_{\text{cut}}$ . In addition, the softening parameter  $r_{\text{cut}}$  leads to a more “collisionless” situation.

As is known, the latter  $N$ -body models suffer from graininess due to the finite number of particles. The graininess manifests itself as a numerical “noise” in the calculation. The use of many model particles  $N \gtrsim 10^4$  decreases drastically the noise level.

Although the direct integration method sounds simple and straightforward, practical computational limitations require the use of only few ten thousands representative stars. This is because we evaluate the sum on the right-hand side of Eq. (1) for each star or  $N$  times for  $N$

stars. The sum itself contains  $N$  terms; each term requires a number of arithmetic operations — for the sake of estimating, let us say, ten. The total number of arithmetic operations required to evaluate the force will be of the order of  $10 \times N^2$ . For the standard Runge–Kutta calculation involving 30,000 stars the total number of operations would be about  $4 \times 10^{10}$ . Assuming that we can do an operation in  $10^{-8}$  sec, simply evaluating the forces would require about 6 – 7 min. A typical calculation requires several thousand time steps so that  $\sim 1,000$  h would be required. Calculations of this magnitude are totally impractical for using such models to explore the physics of galaxies. The problem is solved by using the nowadays concurrent supercomputers: with the multiple processors in supercomputers it is possible to reduce the running time by processing more than one group of particles at a time. The use of, say, 100 parallel computers would make such calculations practical. In the present study, we explore the Inter University 112 processors SGI Origin 2000 supercomputer in Israel.

Note that PIC codes only formally utilized a larger number of particles than direct integration codes. This is because in PIC experiments, the disk plane was covered with a difference grid. The stars within grid cells as well as within a whole model did not interact gravitationally; the computation of the mass density in cells followed a fast Fourier transform to obtain the potential only at a restricted set of points — at the cell centers — by interpolation rules and thus to find the very approximate forces at the positions of the particles. This avoids the need to compute forces between particle pairs, and makes the amount of computation necessary to obtain the forces independent of  $N$ . Clearly, nothing similar exists in nature, and therefore it follows that one cannot compare the number of particles used in these different kinds of simulations in any way at all. Modern parallel computing technology on concurrent processors had led to a dramatic increase in the computing power. The latter allows us to use direct integration methods with a sufficiently large number of model stars  $N = 30,000$ .

### 3. Numerical model

In general, the numerical procedure is first to seek stationary solutions to the Boltzmann kinetic equation in the self-consistent field approximation for the density distribution, the angular velocity of regular rotation, the dispersion of random velocities of the stars, and then to calculate the stability of those solutions to small-amplitude gravity perturbations.

At the start of the  $N$ -body integration, our simulation initializes the particles on a set of 100 circular rings with a circular velocity  $V_{\text{rot}}$  of galactic rotation in the  $r, \varphi$ -plane; the system is isolated in vacuum. Consider an uniformly rotating model disk of stars with a surface mass density variation given by

$$\sigma_0(r) = \sigma(0)\sqrt{1 - r^2/R^2}, \quad (2)$$

where  $\sigma(0)$  is the central surface density and  $R$  is the radius of the initial disk. As a solution of a time-independent collisionless Boltzmann equation, to ensure initial equilibrium the uniform angular velocity to balance the zero-velocity-dispersion disk,

$$\Omega_0 = \pi\sqrt{G\sigma(0)/2R}, \quad (3)$$

was adopted (Hohl, 1971, 1972). Then the position of each particle was slightly perturbed by applying a pseudorandom number generator. For the uniformly rotating disk, the Maxwellian-distributed random velocities with radial  $c_r$  and azimuthal  $c_\varphi$  dispersions in the plane  $z = 0$  according to the familiar Toomre's criterion (Toomre, 1964, 1977) ,

$$c_T = \frac{3.36\sigma_0}{\kappa} = 0.341\Omega_0\sqrt{R^2 - r^2}, \quad (4)$$

may be added ( $c_r = c_\varphi$ ) to the initial circular velocities  $V_{\text{rot}} = r\Omega_0$ , where  $\kappa = 2\Omega[1 + (r/\Omega)(d\Omega/dr)]^{1/2}$  is the ordinary epicyclic frequency (Hohl, 1971, 1972). It is crucial to realize that in this case, according to Lau and Bertin (1978), Lin and Lau (1979), Bertin (1980), Lin and Bertin (1984), Morozov (1980), Polyachenko (1989), Griv and Peter (1996), Polyachenko and Polyachenko (1997), initially the disk is Jeans-stable against the small-scale axisymmetric (radial) perturbations but unstable against the relatively large-scale nonaxisymmetric (spiral) perturbations. The initial vertical velocity dispersion was chosen equal to  $c_z = 0.2c_r$ . Finally, the angular velocity  $\Omega_0$  was replaced by (Hohl, 1971, 1972)

$$\Omega = \left\{ \Omega_0^2 + \frac{1}{r\sigma(r)} \frac{\partial}{\partial r} [\sigma(r)c_r^2(r)] \right\}^{1/2}.$$

The sense of disk rotation was taken to be counterclockwise, and units are such that  $G = 1$  and the mass of a star  $m_s = 1$ . The cutoff radius was chosen  $r_{\text{cut}} = 0.01R$ . Within the framework of our model, dynamically young stars form the very thin disk  $h \ll R$ . Therefore, at the start of simulations the disk thickness was chosen  $h = 0.05R$ . A time  $t = 1$  is taken to correspond to a single revolution of the initial disk. In all experiments the simulation was performed up to a time

$t$  between 8 and 10. It should be noted here that after about three rotations the picture is always stabilized and practically no significant changes in gross properties of the model over this time are observed. Any difference between the results of simulations with and without applying the so-called quiet starts procedure to select the very regular initial coordinates of particles was not found. (Basically, by applying the method of quiet starts, one uses no random numbers in the initial conditions to suppress the noise level in a system. Such techniques have proven useful in obtaining realistic noise levels without the use of a large number of particles; Byers and Grewal, 1970.) Moreover, tests indicated that the results were insensitive to changes in other parameters, e.g. the number of stars in the range  $N = 10,000 - 40,000$ , the cutoff parameter in the range  $r_{\text{cut}} = (0.005 - 0.05)R$  and the initial disk thickness in the range  $h = (0 - 0.2)R$ . Spiral amplitudes detected in our simulations are greatly in excess of an expectation from the level of particle noise and do not scale with  $N$ . This behavior is clearly inconsistent with the hypothesis that the nonaxisymmetric structure in the models can be attributed to collisional effects, inappropriate values of  $r_{\text{cut}}$  or swing-amplified particle noise as advocated by Toomre (1990).

Finally, slight corrections have been applied to the resultant velocities and coordinates of the model stars so as to ensure the equilibrium between the centrifugal and gravitational forces, to preserve the position of the disk center of gravity at the origin and to include the weak effect of the finite thickness of the disk to the gravitational potential. Thus, the initial model is very near the dynamical equilibrium for all radii.

The system of equations of motion (1) for  $N$  particles was integrated by the standard Runge–Kutta method of the fourth order. All the particles move with the same constant Runge–Kutta time step  $\Delta t = 0.001t_{\text{orb}}$ , where  $t_{\text{orb}}$  is the orbital period.

## 4. Results

### 4.1. COLLISIONS

In order to be compared with an actual galaxy of stars, the numerical model of the disk should properly simulate a collisionless system. Otherwise, as it has been shown, e.g. by Morozov *et al.* (1985) and Griv *et al.* (2000a), a collisional disk is unstable with respect to a secular dissipative-type instability. The secular instability of spontaneous gravity perturbations might arise merely from the dissipation of the energy of regular rotation into ever larger amounts of heat when the system has

moderate dissipation; it results from perturbations which have negative energy in the dissipative medium (Morozov *et al.*, 1985; Fridman and Polyachenko, 1984, Vol. 2, p. 243). The secular instability produces structures completely unrelated to the effects we would like to model. In the spirit of the simple “molecular-kinetic” theory by Chandrasekhar (1960), the collisional relaxation time for a three-dimensional system from the point of view of deflections suffered by a test star in encounters with a given distribution of field objects is

$$\tau \approx \frac{c^3}{2\pi G^2 m_f^2 n_f \ln \Lambda_N}, \quad (5)$$

where  $c$  is the averaged velocity dispersion,  $m_f$  is the “field” particle mass and  $n_f$  its three-dimensional number density. Also  $\ln \Lambda_N$  is the so-called Newton (or Coulomb in plasmas) logarithm, by means of which the long-range nature of the gravitational force is taken into account; to the order of magnitude  $\ln \Lambda_N \sim \ln N_f$ , where  $N_f$  is the total number of field particles. In actual galaxies  $\ln \Lambda_N \approx 20$ . According to Eq. (5), the chosen quantities  $c$ ,  $N$ , etc. guarantee that the model may be considered as a collisionless one to a good approximation at least during  $\sim 50$  rotations. So we expect, in our numerical calculations because  $N$  is large, relaxation from two-body gravitational interactions is unimportant. We suggest that the structures observed in the  $N$ -body simulations originate from the collective modes of practically collisionless galactic models — gravitational Jeans-type modes and bending firehose-type modes (see below Section 4.2).

Consider a system of mutually gravitating particles. The local distribution function  $f(\mathbf{r}, \mathbf{v}, t)$  must satisfy the Boltzmann kinetic equation

$$\frac{\partial f}{\partial t} + \mathbf{v} \cdot \frac{\partial f}{\partial \mathbf{r}} - \nabla \Phi \cdot \frac{\partial f}{\partial \mathbf{v}} = \left( \frac{\partial f}{\partial t} \right)_{\text{coll}}, \quad (6)$$

where  $\Phi(\mathbf{r}, t)$  is the total gravitational potential determined self-consistently from the Poisson equation,

$$\nabla^2 \Phi = 4\pi G \int f d\mathbf{v}, \quad (7)$$

$(\partial f / \partial t)_{\text{coll}} \propto \nu_c (f_0 - f)$  is the so-called collisional integral which defines the change of  $f$  arising from ordinary interparticle collisions,  $\nu_c$  is the collision frequency and  $f_0$  is the quasi-steady state distribution function (Binney and Tremaine, 1987, p. 506; Griv *et al.*, 2000a).

In plasma physics, Lifshitz and Pitaevskii (1981, p. 115) have discussed phenomena in which interparticle collisions are unimportant, and such a plasma is said to be collisionless (and in the lowest-order



approximation of the theory one can neglect the collision integral in the kinetic equation). It was shown that a necessary condition is that  $\nu_c \ll |\omega|$ , where  $\omega$  is the typical frequency of collective oscillations: then the collision operator in the kinetic equation is small in comparison with  $\partial f/\partial t$ . In the Appendix, we have shown that the frequency of Jeans oscillations in a stellar disk  $\omega \sim \Omega$ . Therefore, in the gravitation case in the lowest-order approximation of the theory we can neglect the effects of collisions between particles on a time scale of many rotations if  $\nu_c \ll \Omega$ . Lifshitz and Pitaevskii have pointed out that collisions may be neglected also if the particle mean free path is large compared with the wavelength of collective oscillations. Then the collision integral in Eq. (6) is small in comparison with the term  $\mathbf{v} \cdot (\partial f/\partial \mathbf{r})$ .

In this subsection, we test numerically if the models used in our  $N$ -body simulations are being correctly modeled as collisionless Boltzmann (Vlasov) systems. The direct method of checking if the system is being modeled as a collisionless system is to repeat a calculation using a mass spectrum (Rybicki, 1971). It is obvious that as a result of gravitational collisions there is a tendency towards energy equipartition between the various masses. Hohl (1973) has determined the experimental relaxation time and compared it with a theoretical prediction for the collisional relaxation time of a two-dimensional disk. Here we do such a comparison by using the three-dimensional system.

Let us consider the three-dimensional computer model consisting of 2% stars of mass  $m_3 = 10m_s$ , 18% stars of mass  $m_2 = 2m_s$  and 80% stars of mass  $m_1 = 0.55m_s$ . The total number of stars, which are distributed in the system in accord with the law (2) is  $N = 20,000$ . Initially, the different mass groups of stars are distributed with the same velocity dispersion (with different temperatures).

In the Appendix of the present paper we demonstrate that the disk becomes almost stable gravitationally for  $c_r \gtrsim 2c_T$ . In such a Jeans-stable system collective effects associated with the classical gravitational instability will not affect the random velocity dispersion of particles: then the change of velocity dispersion can be explained only by usual two-body encounters. For this reason the initial condition was chosen to be a quasi-stable uniformly rotating disk with  $c_r = 2c_T$ . Following Chandrasekhar (1960) and Hohl (1973), let us define the relaxation time  $\tau_E$  as the time required for the mean change of the kinetic energy per unit mass of the test star to equal the initial kinetic energy.

In Figure 1 we show the change of the ratio of the mean particle (kinetic) energy,  $\langle m_1 V_1^2 \rangle$ ,  $\langle m_2 V_2^2 \rangle$  and  $\langle m_3 V_3^2 \rangle$  (in units of the total kinetic energy of the system), for the different mass groups, where  $V_i$  is the total velocity of a given mass group. As is expected, the



*Figure 1.* Rate of change of the mean kinetic energy for stars of the three mass groups of the Jeans-stable model with  $N = 20,000$  and  $c_r = 2c_T$ ; 1 — kinetic energy of stars with the mass of a star  $10m_s$ , 2 — with the mass of a star  $2m_s$  and 3 — with the mass of a star  $0.55m_s$ . The two groups of heavy stars lose kinetic energy while the group of lightest stars gains an approximately corresponding amount of kinetic energy. In general agreement with the analytical estimation, the mean slope of the curves will result in energy equipartition after about 100 – 200 rotation periods. This result shows that the model used in our  $N$ -body simulations is “collisionless” to a good approximation and suggests that interparticle collisions do not play a significant role for instabilities studied in the paper.

two groups of heavy stars lose energy while the group of lightest stars gains an approximately corresponding amount of kinetic energy. Also as is expected, one can see the decrease in the change of the kinetic energy with time. This is because the collisional frequency  $\nu_c \approx 1/\tau_E$  is inversely proportional to the velocity dispersion (Eq. [5]), and thus the encounters only weakly affect the stars with high random velocities.

As one can see, the mean slope of the curves shown in Figure 1 will result in energy equipartition after about 100 – 200 rotation periods. It is crucial to realize that these relaxation times even for this relatively small number of model stars are much longer than the time of a single disk revolution. We conclude that the computer models used in the present study may be considered as collisionless ones to a good approximation at least during the first 10 rotations which are of especial interest in spiral-galaxy simulation. Therefore, we argue that the collective effects studied in the paper were apparent before the collisional time scale associated with the binary interactions of stars was reached.

#### 4.2. WARM TOOMRE-STABLE DISK

To study the development of spiral structure and to confirm the theoretical predictions made in the Appendix, warm disks with initial radial velocity dispersion of identical stars equal to Toomre’s (1964) stabilizing velocity dispersion  $c_T$  were modeled. Figure 2 shows an example of the development of spiral structures. The structure grows rapidly on a dynamical time scale  $\sim \Omega^{-1}$ . At a time  $t \approx 0.6$  a multi-armed filamentary spiral structure forms with several short, tightly wound



Figure 2a. The time evolution of a warm Toomre-stable three-dimensional disk of stars. The system is violently unstable to low- $m$  spiral Jeans-type modes. After  $\sim 3$  rotations the spiral structure almost disappears, and a prominent bar forms.



Figure 2b. Continued

trailing arms.<sup>1</sup> Soon after, at  $t \approx 2.8$  a bar structure appears with two almost symmetrical open spiral arms. However, sometimes, e.g. at  $t = 1.6$  or at  $t = 2.6$ , one can see a “one-armed” galaxy consisting of a prominent arm and a short, diffuse second one. After  $\sim 3$  rotations, the spiral arms almost disappear, and a bar forms in the central parts of the system.

The  $m = 1$  instability shifts the point with highest density from the center of mass. It is interesting to note that in many disk-shaped galaxies, e.g. in the spiral galaxies M 101 and NGC 1300, there appears to be a deviation from rotational symmetry. In principle, such a deviation may be due to this one arm instability. Note that the latter has already been suggested by B. Lindblad (see Toomre, 1996). In fact, asymmetries in the distribution of light in spiral galaxies have been known for a long time. Baldwin *et al.* (1980) presented a number of spiral galaxies in which the distribution of neutral gas is lopsided, i.e. the gas extends further out on one side of the galaxy than on the other. In many systems asymmetries are also found to be well developed in the stellar disks as indeed confirmed recently by near-infrared observations (Zaritsky and Rix, 1997). Rudnick and Rix (1998) quantified the mean asymmetry of 54 early-type disk galaxies using the amplitude of the  $m = 1$  azimuthal Fourier component of the  $R$ -band surface brightness. It was found that 20% of all disk galaxies have azimuthal asymmetries in their stellar disk distribution, confirming lopsidedness as a dynamical phenomenon. Based on the  $N$ -body simulations, we can offer a tentative hypothesis which accounts lopsided asymmetries in spiral galaxies by the  $m = 1$  Jeans-unstable spiral mode.

Following Athanassoula and Sellwood (1986), in Figure 3 the time evolution of the Fourier spectrum of the spiral pattern shown in Figure

<sup>1</sup> Interestingly, according to fairly recent observations, such ragged galaxies with almost chaotic-looking, “floculent” spiral structures are more common than the grand design ones (Binney and Tremaine, 1987, p. 391).



Figure 3. The time evolution of the Fourier spectrum of the particle distribution shown in Figure 2 for different azimuthal mode numbers  $m$ . In this figure, the ordinate is the Fourier coefficient  $A(p, m)$  and the abscissa is the pitch angle  $p$ . Spiral amplitudes are greatly in excess of an expectation from the level of particle noise  $\sqrt{\pi/4N}$ ; true instabilities develop in the model. The result suggests that very flat stellar disks of galaxies can be unstable to the most unstable one-armed ( $m = 1$ ), two-armed ( $m = 2$ ) and three-armed ( $m = 3$ ) spiral Jeans-type gravity perturbations. The one-armed mode may explain the asymmetric patterns observed in many isolated galaxies.

2 is plotted. Only the azimuthal  $m = 1 - 6$  components are shown. The complex Fourier coefficients,  $A$ , are determined from the following summation

$$A(p, m) = \frac{1}{N} \sum_{j=1}^N \exp\{i[m\varphi_j + p \ln(r_j)]\},$$

where  $N$  is the number of particles and  $(\varphi_j, r_j)$  are the polar coordinates of the  $j$ -th particle. The pitch angle of an  $m$ -armed logarithmic spiral  $\psi$  is given by  $\psi = \arctan(p/m)$ , and positive  $p$  corresponds to trailing spirals and negative  $p$  to leading ones.

This logarithmic spiral Fourier analysis shows that the peaks of the signals move to positive  $p$  with increasing time, reach maxima at  $t = 1.0 - 1.4$ , and eventually decay. It follows, then, that after a time  $t = 2.0 - 3.0$  the model becomes practically stable with respect to gravitational Jeans-type modes. We can observe that the  $m = 1 - 3$  modes are the most unstable ones. An interesting feature is that all these modes have roughly the same pitch angle. The amplitudes of the signals grow aperiodically, supporting the assumption that we have dealt with the aperiodic Jeans-type instability of gravity disturbances.

In actual galaxies, discrete spiral modes were already found by Rix and Zaritsky (1995), Block and Puerari (1999) and Block *et al.* (1999). It was stated that in the near-infrared, the morphology of older star-dominated disk indicates a simple classification scheme: the dominant Fourier  $m$ -mode in the dust penetrated regime, and the associated pitch angle. A ubiquity of low  $m = 1$  and  $m = 2$  modes was confirmed. Fridman *et al.* (1998) detected  $m = 1 - 8$  spiral modes in relatively young stellar population of the nearly face-on galaxy NGC 3631 from observations in the  $H_\alpha$  line.

From the edge-on view pictured in Figure 4, one can see that from an initial very thin model, a fully three-dimensional disk develops



Figure 4a. Higher-resolution plots of the central parts (edge-on view) for the simulation run seen in Figure 2. At a time  $t \approx 1.4$ , one can see the rapid development of the snake-shaped, bending firehose-type instability as a precursor of galactic bulge formation in the central, rigidly rotating portions of the system. This instability is a transient one, and develops on a time scale of single rotation of the system only. The linear dimension of the bending along the  $z$ -axis is comparable to the disk thickness and much less than the radius of the outermost parts of the system. The usual name for this instability of collective systems — firehose instability — recalls the fact that the unstable motion of a hose when the flow velocity of water inside becomes very high has essentially the same nature.



Figure 4b. Continued

immediately at  $t \approx 0.4$  with a mean height  $\langle z \rangle$  above the plane, corresponding to the force balance between the gravitational attraction in the plane and the “pressure” due to the velocity dispersion (i.e. “temperature”) in the vertical,  $z$ -direction. A straightforward estimate shows that

$$\langle z \rangle \approx \frac{c_z}{\sqrt{4\pi G\mu}}, \quad (8)$$

where  $\mu$  is the three-dimensional mass density in the mid-plane. After a time  $t \approx 0.4$  there is no change in the edge-on structure until at  $t \approx 1.4$  (when the Jeans instability is almost switched off by increasing the planar velocity dispersion). At somewhat later times,  $t \approx 3.2$ , a “box-shaped” or “peanut-shaped” bar structure is developed. The development of the box/peanut bar structure is explained in the terms of the bending firehose-type instability (Raha *et al.*, 1991; Merritt and Sellwood, 1994; Griv and Chiueh, 1998).

One sees that at times  $t = 1.4 - 2.4$ , the bending instability fiercely develops in the central, almost rigidly rotating parts of the system and is switched off at  $t \approx 2.8$ . At later times, no dramatic evolution is observed in our simulations. To emphasize, this type of bending instabilities develops in the central, rigidly rotating parts of the system. The three-dimensional simulations show that the bending instabilities mentioned above destroy the strong bar formation (Griv and Chiueh, 1998). Note that the bending modes have been found experimentally by Merritt and Hernquist (1991) and Merritt and Sellwood (1994), but in the nonrotating models. Combes *et al.* (1990) and Raha *et al.*

(1991) found the bending instability in the central regions of a fast-rotating  $N$ -body disk. It was stated that this instability may play a part in the formation of triaxial bulges in flat galaxies and explanation was given why many bulge stars are less than 10 Gyr old (Raha *et al.*, 1991). Bureau and Freeman (1997) have argued that new observations constitute a strong case in favor of the bending (or bar-buckling) mechanism for the formation of boxy/peanut-shaped bulges in spiral galaxies. Observations suggest very strongly that many of ordinary spiral galaxies, including the Milky Way, have similar small triaxial bars in their central regions (Dwek *et al.*, 1995).

Apparently, this instability of a sufficiently thin stellar disk has been predicted by Toomre (1966) by using the simplified theory based on moment equations. Toomre considered the collisionless analog of the Kelvin–Helmholtz instability in an infinite, two-dimensional, nonrotating sheet of stars. This is the usual way to discuss the conditions of the firehose instability in plasma physics (Krall and Trivelpiece, 1986). It was demonstrated by Toomre that the bending instability is driven by the stellar “pressure” anisotropy: the source of free energy in the instability is the intrinsic anisotropy of a velocity dispersion (“temperature”). The bending firehose-type instability was also discovered independently by Kulsrud *et al.* (1971) and Mark (1971) with a more accurate kinetic theory. Kulsrud *et al.* have described the mechanism of the instability in terms of the balance of centrifugal force acting on the stars of a bending layer and the gravitational attraction toward the plane of the practically nonrotating, pressure-supported disk. Fridman and Polyachenko (1984) have discussed the role of the instability in explaining the existence of maximum oblateness in almost nonrotating elliptical galaxies and the formation of the bulges of disk-shaped galaxies of stars.

As is seen in Figures 2 and 4, the basic form of warm disk evolution is the expansion of the outermost parts together with the contraction of a large part of the mass towards the center; in the final quasi-steady state the surface density decreases exponentially outwards (Fig. 5). In a future publication we intend to explain the exponential surface density distribution of the final quasi-steady state model by applying the quasi-linear theory of a stellar disk’s stability. Note only that the study of surface photometry have been shown that most spiral and S0 galaxies have an exponential disk with radial surface-brightness distribution  $\sim \exp(-\text{const} \cdot r)$  (Freeman, 1970).

At first, the surface density and rotation velocity change rapidly (Figs. 5 and 6), but after a time  $t \sim 1.0$  there is little further change during the following two rotations, except in the central portions of the disk. The model generates a nonflat rotation curve (Fig. 6); in addition

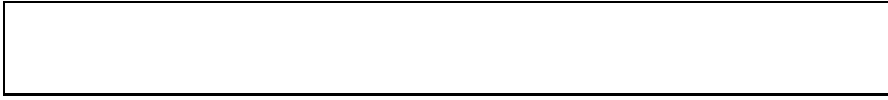


*Figure 5.* Variation of the surface density for a disk shown in Figure 2. Note the rapid change with time of the surface density at  $t < 1$ . The basic form of the disk evolution is the expansion of the outermost portions together with the contraction of a large part of the mass towards the center. In a quasi-steady state after about 2 – 3 rotations, the surface density decreases exponentially outwards. According to observations, stellar disks of most spiral and S0 galaxies are similar approximated well by a function that is exponential in  $r$ .



*Figure 6.* The azimuthal average rotation curve for a stellar disk shown in Figure 2. Note the non-flat rotation curve at the periphery of the system; growing density waves (spiral arms) transfer the angular momentum of the circular motion outwards.

growing density waves (spiral arms) transfer the angular momentum of the circular motion outwards (see the difference in the rotation curves at  $t = 1.0$  and  $t = 2.0$  in Figure 6). As mentioned above, the model practically shows no the time evolution of the surface density and the velocity curve after  $t \approx 2$ . The latter seem to indicate that at that time the system has nearly reached a quasi-steady state (cf. Hohl, 1971).

The time evolution of the velocity dispersions  $c_r$ ,  $c_\varphi$  and  $c_z$  is shown in Figure 7.

Initially, during the first rotation the velocity dispersions along each axis are changed rapidly. During the following two rotations the velocity dispersions are changed with time slightly, confirming that between  $t = 2$  and  $t = 3$  the system has nearly reached a quasi-steady state. However, in the central portions of the disk the velocity dispersion



*Figure 7.* Variation of velocity dispersions for a disk shown in Figure 2; 1 — radial velocity dispersion, 2 — azimuthal velocity dispersion and 3 — vertical velocity dispersion. Initially, during the first rotation the velocity dispersions increase with time rapidly; later the dispersions grow only slightly. However, in the central portions of the disk the vertical velocity dispersion  $c_z$  grows rapidly even after the time  $t \approx 1.5$ , when the bending firehose-type instability begins to operate (see Figure 4). In this central region the bending instability strongly changes the ratio of vertical to radial (and tangential) dispersion by transferring kinetic energy of plane random motions of particles to vertical motions.



Figure 8. Comparison of Toomre's radial-velocity dispersion and the modified critical dispersion with the experimental radial velocity dispersion of a disk shown in Figure 2 at  $t = 2.5$ ; 1 — the experimental radial velocity dispersion, 2 — the modified velocity dispersion, 3 — Toomre's velocity dispersion.



Figure 9. The time development of the mean-square spread in planar random velocity  $v_{\perp}^2$  of model particles for different radii  $r$ .

$c_z$  increases rapidly even after the time  $t \approx 1.5$ , when the bending instability begins to operate.

As was stated, one of the goals of the present research is to compare Toomre's (1964) critical dispersion (4) and the modified dispersion given by Eq. (25) with the experimental radial velocity dispersion of the quasi-steady state model of a stellar disk. In what follows, we are doing such a comparison.

As is seen in Figure 8, the modified critical dispersion, in contrast to Toomre's (1964) critical dispersion, is in fair agreement with the experimental data, especially for the outer, differentially rotating parts of the disk. The agreement is quite reasonable considering the rough nature of the theory. In the central parts of the model the agreement with the theory is not good. This is to be expected since the condition of nearly circular orbits adopted in the Appendix does not fulfill in the central almost nonrotating regions of model disks (and in spiral galaxies, including both barred and normal galaxies, and in disks of elliptical galaxies). Therefore in the central parts of the disk ( $r \lesssim 0.4 - 0.5$ ) the condition for the local criteria (both the Toomre and the modified criterion) to be applicable is violated.

One of the important problems of stellar disks is the determination of the random velocity diffusion. Such velocity diffusion can be caused by stellar disk turbulence. Velocity diffusion produced by turbulence tells us something about the turbulence process.

To compute velocity diffusion we calculate the mean-square spread in the planar random (residual) velocity  $v_{\perp}^2 = c_r^2 + c_{\phi}^2$  as a function of time of model particles for different radii  $r$ . In general  $v_{\perp}^2$  has a time dependence like that shown in Figure 9.

As is seen, in the differentially rotating ( $r > 0.4 - 0.5$ ), Jeans-unstable (at times  $t \lesssim 1.8 - 2.0$ ) parts of the disk approximately  $v_{\perp}^2 \propto$





Figure 10. The time evolution of a hot three-dimensional disk of stars. The system is stable to all Jeans modes. The result agrees with the theoretical explanation described in the paper.

*t.* This behavior has been predicted analytically (see the Appendix). Interestingly, observations indicate a similar increase of  $v_{\perp}^2$  with time in the solar neighborhood (Binney and Tremaine, 1987, p. 470; Gilmore *et al.*, 1990).

#### 4.3. HOT JEANS-STABLE DISK

The time evolution of the hot disk was investigated, in which the initial dispersion of random radial velocities of model stars was chosen to be greater than Toomre's critical dispersion, namely,  $c_r = 2c_T$  (see Eq. [24]). For such calculations we obtain plots like those shown in Figure 10. In agreement with the theory, the system becomes gravitationally (Jeans-) stable.

## 5. Appendices

The linear Lin–Shu density wave theory is considered now as well established (Lin and Shu, 1966; Lin *et al.*, 1969; Shu, 1970; Bertin, 1980; Binney and Tremaine, 1987, p. 347; Griv and Peter, 1996; Griv *et al.*, 2000b). However, as soon as the amplitude of the gravity perturbations becomes appreciable a new generation of problems, namely, nonlinear problems, become important. Below we present a quantitative weakly nonlinear theory of the classical Jeans instability of small-amplitude gravity disturbances (e.g. those produced by a barlike structure, a spontaneous perturbation and/or a companion galaxy) in self-gravitating, rapidly rotating stellar disks of flat galaxies.

In the rotating frame of a disk galaxy, the collisionless motion of an ensemble of identical stars in the plane of the system can be described by the Boltzmann equation for the distribution function  $f(\mathbf{r}, \mathbf{v}, t)$  without the integral of collisions (Lin *et al.*, 1969):

$$\begin{aligned} \frac{\partial f}{\partial t} + v_r \frac{\partial f}{\partial r} + \left( \Omega + \frac{v_{\varphi}}{r} \right) \frac{\partial f}{\partial \varphi} + \left( 2\Omega v_{\varphi} + \frac{v_{\varphi}^2}{r} + r\Omega^2 - \frac{\partial \Phi}{\partial r} \right) \frac{\partial f}{\partial v_r} \\ - \left( \frac{\kappa^2}{2\Omega} v_r + \frac{v_r v_{\varphi}}{r} + \frac{1}{r} \frac{\partial \Phi}{\partial \varphi} \right) \frac{\partial f}{\partial v_{\varphi}} = 0, \quad (9) \end{aligned}$$

where  $r, \varphi, z$  are the galactocentric cylindrical coordinates, the total azimuthal velocity of the stars was represented as a sum of the random  $v_\varphi$  and the basic rotation velocity  $V_{\text{rot}} = r\Omega$ , and  $v_r$  is the random velocity in the radial direction. The quantity  $\Omega(r)$  denotes the angular velocity of galactic rotation at the distance  $r$  from the center, and the epicyclic frequency  $\kappa$  varies from  $2\Omega$  for a rigid rotation to  $\Omega$  for a Keplerian one. Random velocities are small compared with  $r\Omega$ . Collisions are neglected here because the collision frequency is much smaller than the cyclic frequency. In the kinetic equation (9),  $\Phi(\mathbf{r}, t)$  is the total gravitational potential determined self-consistently from the Poisson equation (7).

The equilibrium state is assumed, for simplicity, to be an axisymmetric and spatially homogeneous stellar disk. Secondly, in our simplified model, the perturbation is propagating in the plane of the disk. This approximation of an infinitesimally thin disk is a valid approximation if one considers perturbations with a radial wavelength that is greater than the typical disk thickness. We assume here that the stars move in the disk plane so that  $v_z = 0$ . This allows us to use the two-dimensional distribution function  $f = f(v_r, v_\varphi, t)\delta(z)$  such that  $\int f dv_r dv_\varphi dz = \sigma$ , where  $\sigma$  is the surface density. We expect that the waves propagating in the disk plane have the greatest influence on the development of structures in the disk. The latter suggestion is strongly supported by numerical simulations (Hohl, 1978).

The disk in the equilibrium is described by the following equation:

$$\left(2\Omega v_\varphi + \frac{v_\varphi^2}{r}\right) \frac{\partial f_e}{\partial v_r} - \left(\frac{\kappa^2}{2\Omega} v_r + \frac{v_r v_\varphi}{r}\right) \frac{\partial f_e}{\partial v_\varphi} = 0, \quad (10)$$

where  $\partial f_e / \partial t = 0$  and the angular velocity of rotation  $\Omega(r)$  is such that the necessary centrifugal acceleration is exactly provided by the central gravitational force  $r\Omega^2 = \partial\Phi_e / \partial r$ , where  $\Phi_e$  is the axisymmetric equilibrium potential. Equation (10) does not determine the equilibrium distribution  $f_e$  uniquely. For the present analysis we choose  $f_e$  in the form of the anisotropic Maxwellian (Schwarzschild) distribution

$$f_e = \frac{\sigma_e}{2\pi c_r c_\varphi} \exp\left(-\frac{v_r^2}{2c_r^2} - \frac{v_\varphi^2}{2c_\varphi^2}\right) = \frac{2\Omega}{\kappa} \frac{\sigma_e}{2\pi c_r^2} \exp\left(-\frac{v_\perp^2}{2c_r^2}\right). \quad (11)$$

The Schwarzschild distribution function is a function of the two epicyclic constants of motion  $\mathcal{E} = v_\perp^2/2$  and  $r_0^2\Omega(r_0)$ , where  $r_0 = r + (2\Omega/\kappa^2)v_\varphi$ . These constants of motion are related to the unperturbed star orbits:

$$r = -\frac{v_\perp}{\kappa} [\sin(\phi_0 - \kappa t) - \sin \phi_0]; \quad v_r = v_\perp \cos(\phi_0 - \kappa t);$$

$$\begin{aligned}\varphi &= \frac{2\Omega}{\kappa} \frac{v_{\perp}}{r_0 \kappa} [\cos(\phi_0 - \kappa t) - \cos \phi_0]; \\ v_{\varphi} &\approx r_0 \frac{d\varphi}{dt} + r_0 \frac{v_{\perp}}{\kappa} \frac{d\Omega}{dr} \sin(\phi_0 - \kappa t) \approx \frac{\kappa}{2\Omega} v_{\perp} \sin(\phi_0 - \kappa t),\end{aligned}\quad (12)$$

where  $v_{\perp}$ ,  $\phi_0$  are constants of integration,  $v_{\perp}/\kappa r_0 \sim \rho/r_0 \ll 1$ ,  $\rho$  is the mean epicycle radius, and we follow Lin *et al.* (1969), Shu (1970) and Lynden-Bell and Kalnajs (1972), making use of expressions for the unperturbed epicyclic trajectories of stars (12) in the equilibrium central field  $\Phi_e(r)$ . In Eqs. (12),  $r_0$  is the radius of the circular orbit, which is chosen so that the constant of areas for this circular orbit  $r_0^2(d\varphi_0/dt)$  is equal to the angular momentum integral  $M_z = r^2(d\varphi/dt)$ , and  $v_{\perp}^2 = v_r^2 + (2\Omega/\kappa)^2 v_{\varphi}^2$ . Also,  $\varphi_0$  is the position angle on the circular orbit,  $(d\varphi_0/dt)^2 = (1/r_0)(\partial\Phi_e/\partial r)_0 = \Omega^2$ . The quantities  $\Omega$ ,  $\kappa$  and  $c_r$  are evaluated at  $r_0$ . In Eq. (11) the fact is used that as follows from Eqs. (12) in a rotating frame the radial velocity dispersion  $c_r$  and the azimuthal velocity dispersion  $c_{\varphi}$  are connected through  $c_r \approx (2\Omega/\kappa)c_{\varphi}$ . In the Solar vicinity,  $2\Omega/\kappa \approx 1.7$ . The distribution function  $f_e$  has been normalized according to  $\int_{-\infty}^{\infty} \int_{-\infty}^{\infty} f_e dv_r dv_{\varphi} = 2\pi(\kappa/2\Omega) \int_0^{\infty} v_{\perp} dv_{\perp} f_e = \sigma_e$ , where  $\sigma_e$  is the equilibrium surface density. Such a distribution function for the unperturbed system is particularly important because it provides a fit to observations (Lin *et al.*, 1969; Shu, 1970).

We proceed by applying the standard procedure of the quasi-linear (weakly nonlinear) approach (Lifshitz and Pitaevskii, 1981; Alexandrov *et al.*, 1984; Krall and Trivelpiece, 1986) and decompose the time dependent distribution function  $f = f_0(\mathbf{v}, t) + f_1(\mathbf{v}, t)$  and the gravitational potential  $\Phi = \Phi_0(r, t) + \Phi_1(\mathbf{r}, t)$  with  $|f_1/f_0| \ll 1$  and  $|\Phi_1/\Phi_0| \ll 1$  for all  $\mathbf{r}$  and  $t$ . The functions  $f_1$  and  $\Phi_1$  are oscillating rapidly in space and time, while the functions  $f_0$  and  $\Phi_0$  describe the slowly developing “background” against which small perturbations develop;  $f_0(t=0) \equiv f_e$  and  $\Phi_0(t=0) \equiv \Phi_e$ . The distribution  $f_0$  continues to distort as long as the distribution is unstable. Linearizing Eq. (9) and separating fast and slow varying variables one obtains:

$$\frac{df_1}{dt} = \frac{\partial\Phi_1}{\partial r} \frac{\partial f_0}{\partial v_r} + \frac{1}{r} \frac{\partial\Phi_1}{\partial\varphi} \frac{\partial f_0}{\partial v_{\varphi}},\quad (13)$$

$$\frac{\partial f_0}{\partial t} = \left\langle \frac{\partial\Phi_1}{\partial r} \frac{\partial f_1}{\partial v_r} + \frac{1}{r} \frac{\partial\Phi_1}{\partial\varphi} \frac{\partial f_1}{\partial v_{\varphi}} \right\rangle,\quad (14)$$

where  $d/dt$  means the total derivative along the star orbit (12) and  $\langle \dots \rangle$  denotes the time average over the fast oscillations. To emphasize it again, we are concerned with the growth or decay of small perturbations from an equilibrium state.

In the epicyclic approximation, the partial derivatives in Eqs. (13) and (14) transform as follows (Lin *et al.*, 1969; Shu, 1970; Morozov, 1980; Griv and Peter, 1996):

$$\frac{\partial}{\partial v_r} = v_r \frac{\partial}{\partial \mathcal{E}} - \frac{2\Omega}{\kappa} \frac{v_\varphi}{v_\perp^2} \frac{\partial}{\partial \phi_0}; \quad \frac{\partial}{\partial v_\varphi} = \left( \frac{2\Omega}{\kappa} \right)^2 v_\varphi \frac{\partial}{\partial \mathcal{E}} + \frac{2\Omega}{\kappa} \frac{v_r}{v_\perp^2} \frac{\partial}{\partial \phi_0}. \quad (15)$$

To determine oscillation spectra, let us consider the stability problem in the lowest WKB approximation; this is accurate for short wave perturbations only, but qualitatively correctly even for perturbations with a longer wavelength, of the order of the disk radius  $R$ . In this local WKB approximation in Eqs. (13) and (14), assuming the weakly inhomogeneous disk, the perturbation is selected in the form of a plane wave (in the rotating frame):

$$f_1, \Phi_1 = \frac{1}{2} \delta f, \delta \Phi \left( e^{ik_r r + im\varphi - i\omega_* t} + \text{c.c.} \right), \quad (16)$$

where  $\delta f$ ,  $\delta \Phi$  are amplitudes that are constant in space and time,  $m$  is the nonnegative azimuthal mode number (= number of spiral arms),  $\omega_* = \omega - m\Omega$  is the Doppler-shifted wavefrequency and  $|k_r|R \gg 1$  (Lin *et al.*, 1969; Shu, 1970; Griv and Peter, 1996). The solution in such a form represents a spiral wave with  $m$  arms whose shape in the plane is determined by the relation

$$k_r(r - r_0) = -m(\varphi - \varphi_0). \quad (17)$$

With  $\varphi$  increasing in the rotation direction, we have  $k_r > 0$  for trailing spiral patters, which are the most frequently observed among spiral galaxies. A change of the sign of  $k_r$  corresponds to changing the sense of winding of the spirals, i.e. leading ones. With  $m = 0$ , we have the density waves in the form of concentric rings that propagate away from the center when  $k_r > 0$  or toward the center when  $k_r < 0$ .

In Eq. (13) using the transformation of the derivatives  $\partial/\partial v_r$  and  $\partial/\partial v_\varphi$  given by Eqs. (15), one obtains the solution

$$f_1 = \int_{-\infty}^t dt' \mathbf{v}_\perp \frac{\partial \Phi_1}{\partial \mathbf{r}} \frac{\partial f_0}{\partial \mathcal{E}}, \quad (18)$$

where  $f_1(t' = -\infty) \rightarrow 0$ . In this equation making use of the time dependence of perturbations in the form of Eq. (16) and the unperturbed trajectories of stars (12) in the exponential factor occurring in the formula (18), it is straightforward to show that

$$f_1 = -\Phi_1(r_0) \frac{\partial f_0}{\partial \mathcal{E}} \sum_{l=-\infty}^{\infty} \sum_{n=-\infty}^{\infty} l \kappa \frac{e^{i(n-l)(\phi_0 - \zeta)} J_l(\chi) J_n(\chi)}{\omega_* - l\kappa}, \quad (19)$$

where  $J_l(\chi)$  is the Bessel function of the first kind of order  $l$ ,  $\chi = k_* v_\perp / \kappa \sim k_* \rho$ ,  $k_* = k \{1 + [(2\Omega/\kappa)^2 - 1] \sin^2 \psi\}^{1/2}$  is the effective wavenumber,  $\psi$  is the pitch angle of perturbations,  $\tan \psi = k_\varphi / k_r = m / r k_r$ , and we used the expansion

$$\exp(\pm i b \sin \phi_0) = \sum_{n=-\infty}^{\infty} J_n(b) \exp(\pm i n \phi_0)$$

and the usual Bessel function recursion relation  $J_{l+1}(\chi) + J_{l-1}(\chi) = (2l/\chi)J_l(\chi)$ . In Eq. (19), the denominator vanishes when  $\omega_* - l\kappa \rightarrow 0$ . This occurs near corotation ( $l = 0$ ) and other resonances ( $l = \pm 1, \pm 2, \dots$ ). The Lindblad resonances occur at radii where the field  $(\partial/\partial \mathbf{r})\Phi_1$  resonates with the harmonics  $l = -1$  (inner resonance) and  $l = 1$  (outer resonance) of the epicyclic (radial) frequency of equilibrium oscillations of stars  $\kappa$ . Clearly, the location of these resonances depends on the rotation curve and the spiral pattern speed; the higher the  $m$  value, the closer in radius the resonances are located (Lin *et al.*, 1969; Shu, 1970). In this paper, only the main part of the galactic disk is studied which lies sufficiently far from the resonances: below in all equations  $\omega_* - l\kappa \neq 0$ .

In the WKB approximation, the linearized Poisson equation (7) is readily solved to give the improved Lin–Shu expression for the perturbed surface density of the two-dimensional disk (Lau and Bertin, 1978; Lin and Lau, 1979):

$$\sigma_1 = -|k|\Phi_1/2\pi G. \quad (20)$$

On the other hand, integrating Eq. (19) over velocity space  $\int dv_r \int dv_\varphi f_1 = \pi(\kappa/2\Omega) \int_0^\infty f_1 dv_\perp^2 \equiv \sigma_1$ , and equating the result to the perturbed density given by the improved Lin–Shu solution (Eq. [20]), the dispersion relation  $\omega_* = \omega_*(k_*)$  is obtained:

$$\frac{k^2 c_r^2}{2\pi G \sigma_0 |k|} = -\kappa \sum_{l=-\infty}^{\infty} l \frac{e^{-x} I_l(x)}{\omega_* - l\kappa}, \quad (21)$$

where  $|\omega_*| \neq l\kappa$ ,  $I_l(x)$  is a Bessel function of imaginary argument with its argument  $x = k_*^2 c_r^2 / \kappa^2 \approx k_*^2 \rho^2$ . This dispersion relation generalizes the Lin–Shu–Kalnajs one for nonaxisymmetric perturbations ( $\psi \neq 0$ ) propagating in a homogeneous disk excluding the resonance zones ( $\omega_* - l\kappa \neq 0$ ). Analyzing Eq. (21), it is useful to distinguish between two limiting cases: the cases of epicyclic radius that is small compared with wavelength,  $x \lesssim 1$ , and of epicyclic radius that is large compared with wavelength,  $x \gg 1$ . We study the problem when the frequency of disk oscillations is smaller than the epicyclic frequency.

In the opposite case of the high perturbation frequencies,  $|\omega_*| > \kappa$ , the effect of the disk rotation is negligible and therefore not relevant to us. This is because in this “rotationless” case the star motion is approximately rectilinear on the time and length scales of interest which are the wave growth/damping periods and wavelengths, respectively (cf. Alexandrov *et al.*, 1984, p. 113). Thus, the terms in series (19) and (21) for which  $|l| \geq 2$  may be neglected, and consideration will be limited to the transparency region between the turning points in a disk, i.e. between the inner and outer Lindblad resonances. The  $l = 0$  harmonic that defines the corotation resonance dominates in series.

Thus,  $|\omega_*|$  less than the epicyclic frequency of any disk star. In this case, in Eq. (21) function  $\Lambda(x) = \exp(-x)I_1(x)$  starts from  $\Lambda(0) = 0$ , reaches a maximum  $\Lambda_{\max} < 1$  at  $x \approx 0.5$ , and then decreases. Hence, the growth rate of the instability has a maximum at  $x < 1$  (Griv *et al.*, 1999b, Fig. 2 in their paper). In addition, we consider only low- $m$  perturbations (which are important only for the problem of spiral structure): from now on in all equations  $m \sim 1$ .

Using the well-known asymptotic expansions of Bessel functions, the simplified ( $|l| \leq 1$ ) dispersion relation reads

$$\omega_*^2 = \omega_J^2, \quad (22)$$

where  $\omega_J^2 \approx \kappa^2 - 2\pi G\sigma_0|k|F(x)$  is the squared Jeans frequency and  $F \approx 2\kappa^2 e^{-x}I_1(x)/k^2 c_r^2$  is the so-called reduction factor, which takes into account the fact that the wave field only weakly affects the stars with high random velocities. The latter means that the spiral structure is seen more distinctly in objects with the lowest velocity dispersion. In the limit  $x \lesssim 1$ ,  $F(x) \approx (k_*/k)^2[1-x+(3/4)x^2]$  (but, of course, in order to be appropriate for a WKB wave we consider the perturbations with  $|k_r|r \gg 1$ ). In the opposite limit  $x \gg 1$ ,  $F(x) \approx (1/k\rho)^2[1-(1/2\pi x)^{1/2}]$ . Different forms of  $F(x)$  are given by Athanassoula (1984). The aperiodic Jeans instability (gravitational collapse) is possible when  $\omega_*^2 \equiv \omega_J^2 < 0$ . That is, the real part of the frequency of this unstable motion vanishes in a rotating frame. The Jeans instability is driven by a strong nonresonant interaction of the gravity fluctuations with the bulk of the particle population, and the dynamics of Jeans perturbations can be characterized as a fluid-like interaction. Therefore, such an instability, which implies the displacement of macroscopic portions of a gravitating system, may be also analyzed through the use of relatively simple hydrodynamic equations (Lau and Bertin, 1978; Lin and Lau, 1979; Lin and Bertin, 1984). In general, the growth rate of the Jeans instability is relatively high  $|\Im\omega_J| \sim \Omega$ ; perturbations with wavelength  $\lambda_J \approx 2\pi c_r/\kappa$  have the fastest growth rate (Griv *et al.*, 1999a,b; Griv *et al.*, 2000a,b). In the Solar vicinity of the Galaxy,  $\lambda_J = 2 - 3$  kpc.

Equation (22) has two roots which describe two branches of oscillations: long-wavelength,  $x \lesssim 1$ , and short-wavelength,  $x \gg 1$ , Jeans branches. The dispersion law of low- $m$  Jeans oscillations is

$$\omega_{*1,2} = \pm p|\omega_J|. \quad (23)$$

Here  $p = 1$  for Jeans-stable ( $\omega_J^2 > 0$ ) perturbations and  $p = i$  for Jeans-unstable ( $\omega_J^2 < 0$ ) perturbations.

The Jeans perturbations can be stabilized by the random velocity spread. Indeed, if one recalls that such unstable perturbations are possible only when  $\omega_{*1,2}^2 \equiv \omega_J^2 < 0$ , then by using the condition  $\omega_J^2 \geq 0$  for all possible  $k$ , from Eq. (22) a local stability criterion to suppress the instability of arbitrary Jeans-type gravity perturbations can be easily obtained (Griv *et al.*, 1999a,b; Griv *et al.*, 2000b):

$$c_r \gtrsim c_{r,\text{crit}} = c_T \{1 + (2\Omega/\kappa)^2 - 1\} \sin^2 \psi \}^{1/2}, \quad (24)$$

where  $c_r$  is the radial-velocity dispersion,  $c_{r,\text{crit}}$  is the critical radial velocity dispersion and usually in the main part of a disk-shaped galaxy the parameter  $2\Omega/\kappa = 1.5 - 1.7$ . It is clear from this local criterion that stability of nonaxisymmetric Jeans perturbations ( $\sin \psi \neq 0$ ) in a differentially rotating disk ( $2\Omega/\kappa > 1$ ) requires a larger velocity dispersion than Toomre's critical value  $c_T$ . It is only for rigidly rotating disks ( $2\Omega/\kappa = 1$ ) and/or for axisymmetric perturbations ( $\sin \psi = 0$ ) that the critical value of  $c_r$  is  $c_T$ . Hence, the ordinary Toomre's velocity dispersion  $c_T$  should stabilize only small-scale axisymmetric (radial) perturbations of the Jeans type. The differentially rotating disk however is still unstable against relatively large-scale nonaxisymmetric (spiral) modes with  $\psi \neq 0$ , in particular very open modes with  $\psi \gtrsim 45^\circ$ . According to Polyachenko (1989) and Polyachenko and Polyachenko (1997) the marginal stability condition for Jeans perturbations of an arbitrary degree of axial asymmetry has been available since 1965 (Goldreich and Lynden-Bell, 1965), though in a slightly masked form. A relationship exists between Eq. (24) and what Toomre (Toomre, 1981; Binney and Tremaine, 1987, p. 375) called "swing amplification."

Summarizing, for Jeans-stable differentially rotating stellar disks, the critical value of the radial velocity dispersion must be greater than (although of the order of)  $c_T$ . In accordance with Eq. (24),

$$c_M \approx (2\Omega/\kappa)c_T \sim 2c_T \quad (25)$$

might be the "new" Toomre's velocity dispersion to suppress all Jeans perturbations in a stellar disk, including the most dangerous open ones. Note that the destabilizing effect of tangential ( $\psi \neq 0$ ) gravitational forces (pitch angle dependent effect) was first considered by Lau and



Figure 11. The generalized Lin–Shu–Kalnajs dispersion relation of a homogeneous stellar disk in the case  $2\Omega/\kappa = \sqrt{2}$  and  $|\sin\psi| = 1$  for the different radial velocity dispersion values: (a)  $c_r = 0.5c_M$ , (b)  $c_r = 0.8c_M$ , (c)  $c_r = c_M$  and (d)  $c_r = 1.5c_M$ . The solid curves represent the real part of the dimensionless Doppler-shifted wavefrequency  $\nu = \omega_*/\kappa$  of low-frequency ( $|\omega_*| < \kappa$ ) long-wavelength (1) and short-wavelength (2) Jeans oscillations we are interested in. The dashed curves represent the imaginary part of the dimensionless wavefrequency of low-frequency vibrations. The dot-dashed curves represent the wavefrequencies of additional high-frequency ( $|\omega_*| > \kappa$ ) Jeans modes.

Bertin (1978) and Lin and Lau (1979) using a much simpler gaseous approach, and a stability criterion that is similar to Eq. (25) was also derived. Clearly, the criterion (25) is only approximate one. In the present study, we test the validities of this modified criterion for stability of Jeans perturbations in a self-gravitating, infinitesimally thin and almost collisionless disk of stars.

Correspondingly, for Jeans-stable differentially rotating stellar disks, the critical value of the widely used Toomre’s instability parameter  $Q = c_{r,\text{crit}}/c_T$  must be greater than  $2\Omega/\kappa \sim 2$ . (Toomre’s  $Q$ -value is a measure of the ratio of thermal and rotational stabilization to self-gravitation.) Observations already demonstrated that stellar (and gaseous) disks of a large number of galaxies, including Milky Way’s disk, are near the boundary of the gravitational stability with  $Q$  between 2 and  $2\frac{1}{2}$  over a large range of galactic disks (Fridman *et al.*, 1991; Bottema, 1993).

A general impression of how the spectrum of nonaxisymmetric Jeans perturbations behaves in a homogeneous nonuniformly rotating disk can be gained from Figure 11, which shows the dispersion curves in the cases of Jeans-unstable systems ((a) and (b)), a marginally Jeans-stable system (c) and a Jeans-stable one (d) for values of  $l = 0, \pm 1, \pm 2, \pm 3$  (as determined on a computer from Eq. [21]).

In this figure, the ordinate is the effective wavenumber  $k_*$  measured in terms of the inverse epicyclic radius  $\rho$  and the abscissa is  $\nu = \omega_*/\kappa$ , i.e. the dimensionless angular frequency at which the stars meet with the pattern, measured in terms of the epicyclic frequency  $\kappa$ . In general, for fixed wavefrequency  $\nu$  there are two solutions in  $k_*\rho$ , comprising a long-wavelength wave,  $k_*\rho \lesssim 1$ , and a short-wavelength wave,  $k_*\rho > 1$ . A property of the solution (21) is that in a homogeneous system the Jeans-stable modes those with  $c_r > c_M$  are separated from each other by frequency intervals where there is no wave propagation: gaps





Figure 12. The growth rate of the Jeans instability of a homogeneous stellar disk (arbitrary units) in the case  $2\Omega/\kappa = \sqrt{2}$ ,  $r_0 = 8$ ,  $|k_r| = 1$ ,  $\rho = 1$  and  $|\sin \psi| = 1$  for the different values of the azimuthal mode number  $m$ . The growth rates have maxima with respect to the critical mode number  $m_{\text{crit}} \sim 1$ . The low- $m$  spiral modes ( $m < 10$  and  $m \neq 0$ ) are more unstable than the radial ones ( $m = 0$ ) and the high- $m$  ones ( $m \gtrsim 10$ ).

occur between each harmonic (cf. the Bernstein modes in a magnetized plasma).

The growth rate of the Jeans instability of a homogeneous stellar disk  $\Im\omega_J$  as determined on a computer from the expression  $\sqrt{2\pi G\sigma_0|k|F(x)}$  is shown in Figure 12.

As one can see visually in this Figure, the growth rates have maxima with respect to the critical mode number  $m_{\text{crit}} \sim 1$ . It means that of all harmonics of initial perturbation, one perturbation with the maximum of the growth rate and with  $m = m_{\text{crit}}$  will be formed asymptotically in time. The low- $m$  spiral modes ( $m < 10$  and  $m \neq 0$ ) are more unstable than the radial ones ( $m = 0$ ) and the high- $m$  ones ( $m \gtrsim 10$ ). These low- $m$  spiral modes are only important in the problem of galactic spiral structure because in contrast to the high- $m$  modes, they do extend essentially over a large range of the galactic disk (Lin *et al.*, 1969; Shu, 1970; Griv and Peter, 1996).

The shape and the number of spiral arms depend on the equilibrium parameters of a galaxy. For the Galaxy the most probable pattern is that of 1 – 4 arms, the radial distance between the arms being 2 – 4 kpc. Such a pattern corresponds to a spiral wave mode with maximum of growth rate.

Next we substitute the solution (19) into Eq. (14). Taking into account that the terms  $l \neq n$  vanish for axially symmetric functions  $f_0$ , after averaging over  $\phi_0$  we obtain the equation for the slow part of the distribution function:

$$\frac{\partial f_0}{\partial t} = i\pi \sum_{\mathbf{k}} \sum_{l=-\infty}^{\infty} |\Phi_{1,\mathbf{k}}|^2 \frac{\partial}{\partial v_{\perp}} \frac{k_* \kappa}{v_{\perp} \chi} \frac{l^2 J_l^2(\chi)}{\omega_* - l\kappa} \frac{\partial f_0}{\partial v_{\perp}}. \quad (26)$$

As usual in the weakly nonlinear theory (or weak turbulence theory), in order to close the system one must engage an equation for  $\Phi_{1,\mathbf{k}}$ . Averaging over the fast oscillations, we have

$$(\partial/\partial t)|\Phi_{1,\mathbf{k}}|^2 = 2\Im\omega_*|\Phi_{1,\mathbf{k}}|^2, \quad (27)$$

where suffixes  $\mathbf{k}$  denote the  $\mathbf{k}$ th Fourier component.

Equations (26) and (27) form the closed system of weakly non-linear equations for Jeans oscillations of the rotating homogeneous disk of stars, and describe a diffusion in velocity space. The spectrum of oscillations and their growth rate are given by Eq. (21) and  $\approx \sqrt{2\pi G\sigma_0|k|F(x)} \lesssim \Omega$ , respectively. Thus after a time

$$t \sim 1/\Im\omega_* \sim \Omega^{-1}$$

the Jeans-unstable disk will assume the form described by Eq. (17). In the Solar vicinity,  $\Omega^{-1} \approx 2 \cdot 10^8$  yr. A very important feature of the instability under consideration is the fact that it is aperiodic (the real part of the wavefrequency vanishes in a rotating frame we are using).

As an application of the theory we investigate the relaxation of low frequency and Jeans-unstable,  $|\omega_*| < \kappa$  and  $\omega_*^2 < 0$ , respectively, oscillations in the homogeneous galactic disk. Indeed, already in the 1940s it was observed that in the Solar neighborhood the random velocity distribution function of stars with an age  $t \gtrsim 10^8$  yr is close to a Schwarzschild distribution — a set of Gaussian distributions along each coordinate in velocity space, i.e. close to equilibrium along each coordinate. In addition, older stellar populations have a higher velocity dispersion than younger ones. On the other hand, a simple calculation of the relaxation time of the local disk of the Milky Way due to pairwise star–star encounters brings the standard value  $\sim 10^{14}$  yr (Chandrasekhar, 1960; Binney and Tremaine, 1987, p. 489), which considerably exceeds the lifetime of the universe. According to our approach, collisionless collective-type relaxation does play a determining role in the evolution of stellar populations of the Galactic disk.

Evidently, the unstable fluid-like Jeans oscillations must influence the distribution function of the main, nonresonant part of stars in such a way as to hinder the wave excitation, i.e. to increase the velocity dispersion. This is because the Jeans instability, being essentially a gravitational one, tends to be stabilized by random motions (Griv and Peter, 1996). Therefore, along with the growth of the oscillation amplitude, random velocities must increase at the expense of circular motion, and finally in the disk there can be established a quasi-stationary distribution so that the Jeans-unstable perturbations are completely vanishing and only undamped Jeans-stable waves remain: Jeans instabilities are thought to heat disks up to velocity dispersion values of  $\gtrsim c_M$ .<sup>2</sup>

<sup>2</sup> In turn, the Jeans-stable perturbations are subject to a resonant Landau-type instability (Griv *et al.*, 1999b; Griv *et al.*, 2000b). The resonant interaction of stars with the field of the Jeans-stable waves will be accompanied by an additional increase in the velocity dispersion to values  $c_r$  greater than it follows from approximate criterion (25).

In the following, we restrict ourselves to the most “dangerous,” in the sense of the loss of gravitational stability, long-wavelength perturbations,  $\chi^2$  and  $x^2 \ll 1$  (see the explanation after Eq. [21]). Then in Eqs. (21) and (26) one can use the expansions  $J_1^2(\chi) \approx \chi^2/4$  and  $e^{-x}I_1(x) \approx (1/2)x - (1/2)x^2 + (5/16)x^3$ . Equation (26) takes the simple form

$$\frac{\partial f_0}{\partial t} = D \frac{\partial^2 f_0}{\partial v_\perp^2}, \quad (28)$$

where  $D = (\pi/16\kappa^2) \sum_{\mathbf{k}} k_*^2 \Im\omega_* |\Phi_{1,\mathbf{k}}|^2$ , and both  $\Im\omega_*$  and  $\Phi_{1,\mathbf{k}}$  are functions of  $t$ . As is seen, the velocity diffusion coefficient for non-resonant stars  $D$  is independent of  $v_\perp$  (to lowest order). This is a qualitative result of the nonresonant character of the star’s interaction with collective aggregates.

By introducing  $d\tau/dt = D(t)$  and  $d/dt = (d\tau/dt)(d/d\tau)$  (Alexandrov *et al.*, 1984; Krall and Trivelpiece, 1986), Eqs. (27) and (28) are rewritten as follows:

$$\frac{\partial f_0}{\partial \tau} - \frac{\partial^2 f_0}{\partial v_\perp^2} = 0, \quad \frac{\partial D}{\partial \tau} = 2\Im\omega_*, \quad (29)$$

which has the solution

$$f_0(v_\perp, \tau) = \frac{\text{const}}{\sqrt{\tau}} \exp\left(-\frac{v_\perp^2}{4\tau}\right). \quad (30)$$

(We have taken into account the observations that the distribution of newly born stars is close to the  $\delta$ -function distribution,  $f_0(\mathbf{v}_\perp, t = 0) = \delta(\mathbf{v}_\perp)$ ; Grivnev and Fridman, 1990.)

Two general physical conclusions can be deduced from the solution (30). First, during the development of the Jeans instability,  $\Im\omega_* > 0$ , the Schwarzschild distribution of random velocities (a Gaussian spread along  $v_r, v_\varphi$  coordinates in velocity space) is established. In sharp contrast to a normal gas with frequent interparticle collisions, it is the collisionless collective-type interactions between the stars which transform an arbitrary initial distribution into the Maxwellian-like form. Secondly, the energy of the oscillation field  $\propto \sum_{\mathbf{k}} |\Phi_{1,\mathbf{k}}|^2$  plays the role of a “temperature”  $T$  in the nonresonant-particle distribution. As the perturbation energy increases, the initially monoenergetic distribution spreads ( $f_0$  becomes less peaked), and the effective temperature (or  $v_\perp^2$ ) grows with time (a Gaussian spread increases):  $T = 2\tau \propto \int D(t)dt \propto \int \sum_{\mathbf{k}} k_*^2 \Im\omega_* |\Phi_{1,\mathbf{k}}|^2 dt$ . That is, during the development of the Jeans instability the planar mean-square velocity increases linearly with time. In Section 4.2 of the present paper, we verify the  $v_\perp^2 \propto t$  dependence by  $N$ -body simulations.

From the above, this nonlinear wave–star interaction increases the velocity dispersion of stars in Milky Way’s disk after they are born (and of particles in Jeans-unstable  $N$ -body models). Subsequently, sufficient velocity dispersion prevents Jeans’ instability from occurring. The “diffusion” of nonresonant stars takes place because they gain mechanical (oscillatory) energy as the instability develops. The velocity diffusion, however, presumably tapers off as Jeans stability is approached: the radial velocity dispersion  $c_r$  becomes greater than the critical one  $c_M$ . This is large enough to turn off the Jeans instability in a stellar disk. Thus, the true time scale for relaxation in the Milky Way may be much shorter than its standard value  $\sim 10^{14}$  yr for the classical Chandrasekhar–Ogorodnikov collisional relaxation; it may be of the order  $(\mathfrak{S}\omega_*)^{-1} \gtrsim \Omega^{-1} \gtrsim 10^9$  yr, i.e. comparable with 10 periods of the Milky Way rotation in the Solar vicinity. The above relaxation time is in fair agreement with both observations and  $N$ -body simulations of Milky Way’s disk (Binney and Tremaine, 1987, p. 478; Grivnev and Fridman, 1990; Hohl, 1971).

## 6. Summary

The results show that a velocity dispersion given by Toomre’s (1964) criterion will stabilize a disk only against axisymmetric ring-like gravity perturbations. However, such disks are unstable against nonaxisymmetric spiral-like perturbations. Jeans-unstable spiral perturbations “heat” the system; the mean-square random velocity increases linearly with time. The results are in agreement with analytical predictions.

We were able to generate an axisymmetric, gravitationally stable disk. The initial condition for the axisymmetric stable disk was obtained analytically and confirmed experimentally: the radial dispersion of random velocities of stars should be equal (or greater than) to the modified dispersion at each radii.

## 7. Acknowledgements

This work was performed in part under the auspices of the Israeli Ministry of Immigrant Absorption, the Israel–U.S. Binational Science Foundation, the Israel Science Foundation and the Academia Sinica in Taiwan. The authors thank Tzi-Hong Chiueh, Arthur D. Chernin, Alexei M. Fridman and Shlomi Pistinner for their interest in the work and valuable suggestions. In part, this work was done while one of the authors (E. G.) was a Senior Postdoctoral Fellow at the ASIAA during

1996–1997. E. G. would like to thank Yi-Nan Chin, Minhoo Choi, Yi-Jehng Kuan, Jeremy Lim, Kwok-Yung Lo and Jun-Hui Zhao for many useful discussions during his two-year stay, and all the staff of ASIAA for their hospitality.

### References

- ALEXANDROV, A. F., BOGDANKEVICH, L. S. AND RUKHADZE, A. A.: 1984, *Principles of Plasma Electrodynamics*, Springer, Berlin.
- ATHANASSOULA, E.: 1984, Phys. Rep. **114**, 319.
- ATHANASSOULA, E. AND SELLWOOD, J. A.: 1986, Mon. Not. R. astr. Soc. **221**, 213.
- BALDWIN, J. E., LYNDEN-BELL, D. AND SANCISI, R.: 1980, Mon. Not. R. astr. Soc. **193**, 313.
- BERTIN, G.: 1980, Phys. Rep. **61**, 1.
- BINNEY, J. AND TREMAINE, S.: 1987, *Galactic Dynamics*, Princeton Univ. Press, Princeton, NJ.
- BLOCK, D. L. AND PUERARI, I.: 1999, Astron. Astrophys. **342**, 627.
- BLOCK, D. L., PUERARI, I., J. A. FROGEL *et al.*: 1999, Astrophys. Space Sci. **269**, 5.
- BOTTEMA, R.: 1993, Astron. Astrophys. **275**, 16.
- BUREAU, M. AND FREEMAN, K. C.: 1997, Publ. Astron. Soc. Austr. **14**, 146.
- BYERS, J. AND GREWAL, M.: 1970, Phys. Fluids **13**, 1819.
- CHANDRASEKHAR, S.: 1960, *Stellar Dynamics*, Dover, New York.
- COMBES, F., DEBBASCH, F., FRIEDLY, D. AND PFENNIGER, D.: 1990, Astron. Astrophys. **233**, 82.
- DONNER, K. J. AND THOMASSON, M.: 1994, Astron. Astrophys. **290**, 785.
- DWEK, E., ARENDT, R. G., M. G. HAUSER *et al.*: 1995, Astrophys. J. **445**, 716.
- FREEMAN, K. C.: 1970, Astrophys. J. **160**, 811.
- FRIDMAN, A. M., KORUZHII, O. V., A. V. ZASOV *et al.*: 1998, Astron. Lett. **24**, 764.
- FRIDMAN, A. M. AND POLYACHENKO, V. L.: 1984, *Physics of Gravitating Systems*, vols. 1 and 2, Springer, New York.
- FRIDMAN, A. M., POLYACHENKO, V. L. AND ZASOV, A. V.: 1991, in *IAU Symp. 146, Dynamics of Galaxies and Their Molecular Cloud Distribution*, F. Combes and F. Gasoli (eds.), Dordrecht, Kluwer, p. 109.
- GILMORE, G., KING, I. R. AND VAN DER KRUIT, P. C.: 1990, in *The Milky Way as a Galaxy*, R. Buser and I. R. King (eds.), Univ. Science Book, Mill Valley, CA, p. 161.
- GOLDREICH, P. AND LYNDEN-BELL, D.: 1965, Mon. Not. R. astr. Soc. **130**, 125.
- GRIV, E. AND CHIUEH, T.: 1998, Astrophys. J. **503**, 186.
- GRIV, E., CHIUEH, T. AND PETER, W.: 1994, Physica A **205**, 299.
- GRIV, E., GEDALIN, M., EICHLER, D. AND YUAN, C.: 2000a, Planet. Space Sci. **48**, 679.
- GRIV, E., GEDALIN, M., EICHLER, D. AND YUAN, C.: 2000b, Phys. Rev. Lett., **84**, 4280.
- GRIV, E. AND PETER, W.: 1996, Astrophys. J. **469**, 84.
- GRIV, E., ROSENSTEIN, B., GEDALIN, M. AND EICHLER, D.: 1999a, Astron. Astrophys. **347**, 821.
- GRIV, E., YUAN, C. AND GEDALIN, M.: 1999b, Mon. Not. R. astr. Soc. **307**, 1.

- GRIV, E. AND ZHYTNIKOV, V. V.: 1995, *Astrophys. Space Sci.* **226**, 51.
- GRIVNEV, E. M.: 1985, *Soviet Astron.* **29**, 400.
- GRIVNEV, E. M. AND FRIDMAN, A. M.: 1990, *Soviet Astron.* **34**, 10.
- HOCKNEY, R. W. AND BROWNRIGG, D. R. K.: 1974, *Mon. Not. R. astr. Soc.* **167**, 351.
- HOHL, F.: 1971, *Astrophys. J.* **168**, 343.
- HOHL, F.: 1972, *J. Comput. Phys.* **9**, 10.
- HOHL, F.: 1973, *Astrophys. J.* **184**, 353.
- HOHL, F.: 1978, *Astron. J.* **83**, 768.
- HOHL, F. AND HOCKNEY, R. W.: 1969, *J. Comput. Phys.* **4**, 306.
- KRALL, N. A. AND TRIVELPIECE, A. W.: 1986, *Principles of Plasma Physics*, San Francisco Press, San Francisco.
- KULSRUD, R. M., MARK, J. W.-K. AND CARUSO, A.: 1971, *Astrophys. Space Sci.* **14**, 52.
- LAU, Y. Y. AND BERTIN, G.: 1978, *Astrophys. J.* **226**, 508.
- LIFSHITZ, E. M. AND PITAEVSKII, L. P.: 1981, *Physical Kinetics*, Pergamon, Oxford.
- LIN, C. C. AND BERTIN, G.: 1984, *Adv. Appl. Mech.* **24**, 155.
- LIN, C. C. AND LAU, Y. Y.: 1979, *SIAM Stud. Appl. Math.* **60**, 97.
- LIN, C. C. AND SHU, F. H.: 1966, *Proc. Natl. Acad. Sci.* **55**, 229.
- LIN, C. C., YUAN, C. AND SHU, F. H.: 1969, *Astrophys. J.* **155**, 721.
- LYNDEN-BELL, D. AND KALNAJS, A. J.: 1972, *Mon. Not. R. astr. Soc.* **157**, 1.
- MARK, J. W.-K.: 1971, *Astrophys. J.* **169**, 455.
- MERRITT, D. AND HERNQUIST, L.: 1991, *Astrophys. J.* **376**, 439.
- MERRITT, D. AND SELLWOOD, J. A.: 1994, *Astrophys. J.* **425**, 551.
- MILLER, R. H.: 1971, *Astrophys. Space Sci.* **14**, 73.
- MOROZOV, A. G.: 1980, *Soviet Astron.* **24**, 391.
- MOROZOV, A. G.: 1981, *Soviet Astron.* **25**, 421.
- MOROZOV, A. G., TORGASHIN, YU. M. AND FRIDMAN, A. M.: 1985, *Soviet Astron. Lett.* **11**, 94.
- OSTRIKER, J. P. AND PEEBLES, P. J. E.: 1973, *Astrophys. J.* **186**, 467.
- PFENNIGER, D. AND FRIEDLI, D.: 1993, *Astron. Astrophys.* **270**, 561.
- POLYACHENKO, V. L.: 1989, in *Dynamics of Astrophysical Discs*, J. A. Sellwood (ed.), Cambridge Univ. Press, Cambridge, p. 199.
- POLYACHENKO, V. L. AND POLYACHENKO, E. V.: 1997, *J. Exper. Theor. Phys.* **85**, 417.
- QUIRK, W. J.: 1972, in *Gravitational N-body Problem*, M. Lecar (ed.), Reidel, Dordrecht, p. 250.
- ROMEO, A. B.: 1998, *Astron. Astrophys.* **335**, 922.
- RAHA, N., SELLWOOD, J. A., JAMES, R. A. AND KAHN, F. D.: 1991, *Nature* **352**, 411.
- RIX, H.-W. AND ZARITZKY, D.: 1995, *Astrophys. J.* **447**, 82.
- RUDNICK, G. AND RIX, H.-W.: 1998, *Astrophys. J.* **116**, 1163.
- RYBICKI, G. B.: 1971, *Astrophys. Space Sci.* **14**, 15.
- SALO, H.: 1995, *Icarus* **117**, 287.
- SHU, F. H.: 1970, *Astrophys. J.* **160**, 99.
- TOOMRE, A.: 1964, *Astrophys. J.* **139**, 1217.
- TOOMRE, A.: 1966, in *Notes on the Summer Study Programm in Geophysical Fluid Dynamics at the Woods Hole Oceanographic Institution*, p. 111.
- TOOMRE, A.: 1977, *Ann. Rev. Astr. Ap.* **15**, 437.
- TOOMRE, A.: 1981, in *Structure and Evolution of Normal Galaxies*, S. M. Fall and D. Lynden-Bell (eds.), Cambridge Univ. Press, Cambridge.

- TOOMRE, A.: 1990, in *Dynamics and Interactions of Galaxies*, R. Wielen (ed.), Springer, Berlin, p. 292.
- TOOMRE, A. AND KALNAJS, A. J.: 1991, in *Dynamics of Disc Galaxies*, B. Sundelius (ed.), Göteborg Univ. Press, Göteborg, p. 341.
- TOOMRE, A.: 1996, in *Barred Galaxies and Circumnuclear Activity*, Aa. Sandqvist and P. O. Lindblad (eds.), Springer, Berlin, p. 1.
- ZARITSKY, D. AND RIX, H.-W.: 1997, *Astrophys. J.* **477**, 118.
- Address for Offprints:* KLUWER ACADEMIC PUBLISHERS PrePress Department,  
P.O. Box 17, 3300 AA Dordrecht, The Netherlands  
e-mail: TEXHELP@WKAP.NL  
Fax: +31 78 6392500





This figure "griv\_fig1.gif" is available in "gif" format from:

<http://arxiv.org/ps/astro-ph/0011445v1>

This figure "griv\_fig2a.gif" is available in "gif" format from:

<http://arxiv.org/ps/astro-ph/0011445v1>

This figure "griv\_fig2b.gif" is available in "gif" format from:

<http://arxiv.org/ps/astro-ph/0011445v1>

This figure "griv\_fig3.gif" is available in "gif" format from:

<http://arxiv.org/ps/astro-ph/0011445v1>

This figure "griv\_fig4a.gif" is available in "gif" format from:

<http://arxiv.org/ps/astro-ph/0011445v1>

This figure "griv\_fig4b.gif" is available in "gif" format from:

<http://arxiv.org/ps/astro-ph/0011445v1>

This figure "griv\_fig5.gif" is available in "gif" format from:

<http://arxiv.org/ps/astro-ph/0011445v1>

This figure "griv\_fig6.gif" is available in "gif" format from:

<http://arxiv.org/ps/astro-ph/0011445v1>



This figure "griv\_fig7.gif" is available in "gif" format from:

<http://arxiv.org/ps/astro-ph/0011445v1>

This figure "griv\_fig8.gif" is available in "gif" format from:

<http://arxiv.org/ps/astro-ph/0011445v1>

This figure "griv\_fig9.gif" is available in "gif" format from:

<http://arxiv.org/ps/astro-ph/0011445v1>

This figure "griv\_fig10.gif" is available in "gif" format from:

<http://arxiv.org/ps/astro-ph/0011445v1>

This figure "griv\_fig11.gif" is available in "gif" format from:

<http://arxiv.org/ps/astro-ph/0011445v1>

This figure "griv\_fig12.gif" is available in "gif" format from:

<http://arxiv.org/ps/astro-ph/0011445v1>